

SUPPLEMENTARY DATA

Supplementary methods

Cardiac magnetic resonance data acquisition and analyses

All CMR examinations were conducted using 3.0-Tesla systems (Ingenia CX, Philips Healthcare, Best, The Netherlands, and MR750W, General Electric Healthcare, Waukesha, Wisconsin, USA).

Balanced steady-state free precession cine sequences were acquired during breath-hold, encompassing 8 to 12 contiguous short-axis slices from the mitral annulus to the apex alongside standard 2-, 2-, and 4-chamber long-axis views. Critical acquisition parameters included repetition time/echo time (TR/TE) of 3.2/1.6 ms, field of view (FOV) of $350 \times 350 \text{ mm}^2$, slice thickness of 8 mm (short-axis) or 5 mm (long-axis) without inter-slice gaps, 45° flip angle (FA), spatial resolution of $2.0 \times 1.6 \times 8 \text{ mm}^3$, and parallel imaging acceleration factors from 1.5 to 3 optimized for individual breath-hold capacity.

Multishot turbo spin-echo (TSE) sequences generated fat-suppressed T2-weighted black-blood images using TR = 2 cardiac cycles, TE = 75 ms, FA = 90° , resolution of $1.7 \times 1.7 \times 8 \text{ mm}^3$, and acceleration factor=2.

Late gadolinium enhancement (LGE) imaging used inversion-recovery prepared 3D gradient echo sequences initiated 10 minutes postadministration of 0.2 mmol/kg Magnevist (Bayer Healthcare, Germany), with inversion time individually adjusted for myocardial nulling at TR/TE of 4.1/1.6 ms, 20° flip angle, and 256×130 matrix size.

Cardiac magnetic resonance data analysis

Two CMR technologists (QG/RG; 5 years of experience) conducted blinded analyses using CVI42 v5.13 (Circle Cardiovascular Imaging), with final adjudication by a senior cardiologist (HW).

Endocardial and epicardial borders were manually traced across all short-axis cine images to derive indexed left ventricular end-diastolic and end-systolic volumes (LVEDVi/LVESVi), myocardial mass, stroke volume, and ejection fraction following established protocols.

Myocardial strain analysis referenced end-diastolic phases, with contouring of biventricular endo/epicardial borders across all views. Insertion points of right ventricular anterior/inferior walls were manually annotated. Global longitudinal, radial, and circumferential strain (GLS/GRS/GCS) values represented mean peak measurements from standardized 16-segment models.

LGE analysis defined the infarct core as hyperenhanced myocardium exceeding remote myocardium signal by >5 standard deviations (SD), with microvascular obstruction (MVO) identified as central hypoenhancement within these regions. Myocardial edema (area-at-risk, AAR) was quantified as tissue >2 SD above skeletal muscle reference signal, while hypointense zones within AAR indicated intramyocardial hemorrhage (IMH) or persistent iron deposition. Myocardial salvage index (MSI) was calculated as $[(AAR - \text{infarct volume})/AAR] \times 100\%$ per established methodology (PMID: 20129530). All pathology volumes (infarct size, MVO, IMH, iron) were normalized to left ventricular mass (%LV).

In LGE analysis, hyperenhanced regions (> 5 SD above remote myocardium) defined infarct core, with central hypoenhancement indicating microvascular obstruction (MVO). Myocardial edema (area-at-risk, AAR) was quantified as regions > 2 SD above skeletal muscle reference. Intramyocardial hemorrhage (IMH) and persistent iron were identified as hypointense zones within AAR. Myocardial salvage index (MSI) was calculated as $(AAR - \text{infarct volume})/AAR \times 100\%$ [1]. Infarct size, MVO, IMH, and persistent iron were normalized to left ventricular mass (%LV).

Procedures and measurement of angio-IMR

Selective coronary angiography captured at 15 to 30 frames/second included ≥ 2 projections with $\geq 30^\circ$ angular separation without table movement, ensuring adequate opacification of the arterial tree. Acquired Digital Imaging and Communications in Medicine (DICOM) angiography data and post-percutaneous coronary intervention (PPCI) aortic pressure waveforms underwent processing via dedicated software (FlashAngio IMR, Rainmed Ltd., China). Three-dimensional (3D) coronary reconstruction generated a vascular mesh extending from the ostium to distal segments.

Mean aortic pressure (MAP) was determined by averaging 3 consecutive cardiac cycles, with maximal hyperemic MAP $[(P_a)_{hyp}]$ calculated as $MAP \times 0.8$ when $MAP \geq 95$ mmHg or $MAP \times 0.85$ when $MAP < 95$ mmHg[2]. The diastolic flow velocity ($V_{diastole}$) was determined automatically by the FlashAngio IMR software, similar to a previous study.³ Systolic and diastolic phases were determined through real-time tracking of guiding catheter tip motion in angiographic sequences, leveraging its direct connection to the coronary tree. Characteristic oscillatory movement patterns identified systole as the shorter-duration inward/outward displacement interval, with diastole corresponding to the prolonged phase. We computed the diastolic flow velocity by the Thrombolysis in Myocardial Infarction (TIMI) Frame Count Method, i.e., $V_{diastole} = (\text{contrast passing length})/(\text{diastolic time interval})$, where the contrast passing length is the distance that contrast moves in 3D reconstructed coronary arteries during the period of diastole. The maximal hyperemic flow velocity, V_{hyp} , is assumed equal to $2.1 \times V_{diastole}$ [4].

A custom computational fluid dynamics (CFD) model executed steady-state laminar flow simulations across stenotic segments within 10 to 30 seconds.² The CFD method with the inlet velocity

of V_{hyp} was used to solve the Navier-Stokes and continuity equations in the FlashAngio software and compute the pressure drop $((\Delta P)_{hyp})$ along meshed coronary arteries from the inlet to the distal position ($L = 75$ mm downstream from the inlet of the coronary arterial tree) and $(P_d)_{hyp} = (P_a)_{hyp} - (\Delta P)_{hyp}$. The angio-FFR was computed using the equation in the previous study.² The angio-IMR was computed in $angioIMR = (P_a)_{hyp} \cdot angioFFR \cdot \frac{L}{2.1 \cdot V_{diastole}}$, where L is a constant (nondimensional) that mimics the length from the inlet to the distal position ($L = 75$, mimicking 75 mm downstream from the inlet of the coronary tree). All angio-FFR and angio-IMR computations were performed by an independent core laboratory (Beijing Anzhen Hospital, Capital Medical University) under blinded conditions relative to clinical and CMR outcomes. A cutoff of angio-IMR > 40 U was considered indicative of clinically significant microvascular dysfunction in the culprit vessel as previously reported.⁵

Supplementary results

Sensitivity Analyses

When malignant ventricular arrhythmia was excluded from the composite outcome, CMD remained significantly associated with adverse events in patients with MetS (HR = 2.208; 95%CI: 1.187-4.108; $P = .012$), whereas no significant association was observed in those without MetS (HR = 1.502; 95%CI: 0.553-4.079; $P = .425$) (**Table S3**). Furthermore, when both stroke and malignant ventricular arrhythmia were excluded—restricting the endpoint to cardiac death, nonfatal MI, ischemia-driven revascularization, or hospitalization for heart failure—the prognostic association between CMD and adverse outcomes persisted in the MetS group (HR = 2.231; 95%CI: 1.199-4.152; $P = .011$) but not in the non-MetS group (HR = 1.502; 95%CI: 0.553-4.079; $P = .425$) (**Table S3**).

Table S1. CMR findings at baseline

	Overall	MetS			Non-MetS		
		non-CMD	CMD	P	non-CMD	CMD	P
<i>CMR findings during index hospitalization</i>							
Number of patients	497	250	66		135	46	
LVEDVi, mL/m ²	69.35 ± 15.73	68.89 ± 15.49	70.85 ± 14.83	.356	68.33 ± 13.64	72.75 ± 22.54	.114
LVESVi, mL/m ²	34.31 ± 13.49	33.94 ± 13.34	37.25 ± 11.96	.068	32.31 ± 10.62	37.94 ± 20.97	.019
LVEF, %	51.30 ± 11.03	51.47 ± 11.62	48.32 ± 8.37	.040	53.12 ± 10.51	49.32 ± 11.66	.041
LV mass index, g/m ²	68.37 ± 14.34	70.48 ± 13.25	70.31 ± 14.42	.925	63.33 ± 10.01	68.85 ± 24.28	.032
Area at risk, % LV mass	55.74 [42.91, 66.10]	52.50 [39.38, 64.93]	59.94 [48.45, 70.75]	.002	55.13 [43.12, 65.83]	63.80 [53.01, 69.18]	.010
Infarct size, % LV mass	29.36 [20.46, 37.45]	26.13 [18.40, 36.13]	34.94 [26.87, 44.80]	< .001	29.54 [21.08, 36.93]	33.20 [24.44, 42.42]	.032
Myocardial salvage index	24.49 [18.09, 30.30]	23.91 [18.06, 29.98]	24.00 [17.79, 28.25]	.531	25.28 [17.70, 30.86]	25.92 [21.89, 30.34]	.283
Presence of MVO	298 (60.0)	129 (51.6)	54 (81.8)	< .001	79 (58.5)	36 (78.3)	.026
MVO, % LV mass	0.46 [0.00, 3.18]	0.07 [0.00, 2.50]	2.42 [0.41, 5.02]	< .001	0.27 [0.00, 2.29]	1.42 [0.08, 5.88]	.003
Presence of IMH	175 (35.2)	74 (29.6)	35 (53.0)	.001	44 (32.6)	22 (47.8)	.087
IMH, % LV mass	0.00 [0.00, 0.71]	0.00 [0.00, 0.56]	0.44 [0.00, 1.43]	.001	0.00 [0.00, 0.48]	0.00 [0.00, 1.20]	.116

CMD, coronary microvascular dysfunction; IMH, intramyocardial hemorrhage; LV, left ventricular; LVEDVi, left ventricular end diastolic volume index; LVEF, left ventricular ejection fraction; LVESVi, left ventricular end systolic volume index; MetS, metabolic syndrome; MVO, microvascular obstruction; SD, standard deviation.

Data are presented as mean ± standard deviation, median [interquartile range], or No. (%).

Table S2. Cox regression analysis for different endpoints

Endpoint	MetS categories	Variables	Univariable Analysis		Multivariable Analysis*		
			HR (95%CI)	P	HR (95%CI)	P	
Cardiac death, nonfatal MI, stroke, ischemia-driven revascularization, or hospitalization for HF							
	<i>MetS</i>	Angio-IMR	1.010 (1.001-1.019)	.029	1.022 (1.010-1.033)	< .001	
		Non-CMD (angio-IMR ≤40)	Reference	...	Reference	...	
		CMD (angio-IMR > 40)	1.870 (1.103-3.169)	.020	2.208 (1.187-4.108)	.012	
	<i>Non-MetS</i>	Angio-IMR	1.008 (0.989-1.027)	.429	1.008 (0.990-1.025)	.378	
		Non-CMD (angio-IMR ≤ 40)	Reference	...	Reference	...	
		CMD (angio-IMR > 40)	1.016 (0.401-2.577)	.973	1.502 (0.553-4.079)	.425	
Cardiac death, nonfatal MI, ischemia-driven revascularization, or hospitalization for HF							
	<i>MetS</i>	Angio-IMR	1.010 (1.001-1.019)	.037	1.021 (1.010-1.033)	< .001	
		Non-CMD (angio-IMR ≤ 40)	Reference	...	Reference	...	
		CMD (angio-IMR > 40)	1.833 (1.066-3.153)	.028	2.231 (1.199-4.152)	.011	
	<i>Non-MetS</i>	Angio-IMR	0.995 (0.972-1.019)	.675	1.008 (0.990-1.025)	.378	
		Non-CMD (angio-IMR ≤ 40)	Reference	...	Reference	...	
		CMD (angio-IMR > 40)	0.889 (0.326-3.153)	.818	1.502 (0.553-4.079)	.425	

CI, confidence interval; CMD, coronary microvascular dysfunction; IMR, index of microcirculatory resistance; MetS, metabolic syndrome; MI, myocardial infarction; HF, heart failure; HR, hazard ratio.

*Multivariable analysis: adjusted for age, sex, current smoking, prior stroke, location anterior, total ischemic time, number of vessels diseased, and Killip class.

Table S3. CMR findings at follow-up according to the MeS and angio-IMR levels

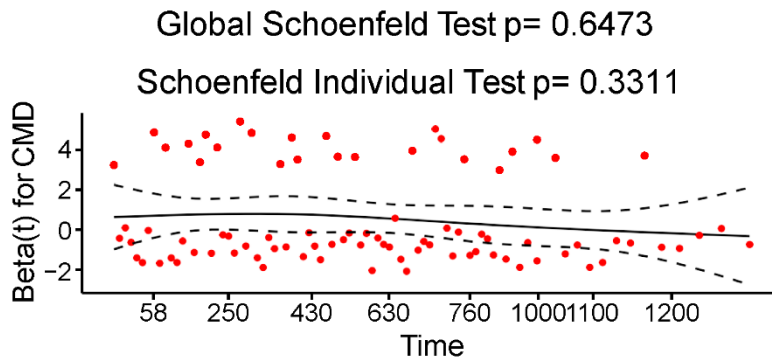
	Overall	MeS			Non-MeS		
		non-CMD	CMD	<i>P</i>	non-CMD	CMD	<i>P</i>
<i>CMR findings at 3 mo</i>							
Number of patients	173	72	34		47	20	
LVEDVi, mL/m ²	73.65 ± 16.74	72.90 ± 14.51	78.37 ± 22.27	.133	72.73 ± 16.38	70.47 ± 13.59	.590
LVESVi, mL/m ²	34.18 ± 14.45	32.97 ± 13.54	39.99 ± 19.13	.032	33.01 ± 12.90	31.43 ± 9.39	.624
LVEF, %	55.03 ± 10.72	56.16 ± 11.62	50.97 ± 10.91	.031	55.83 ± 9.99	56.01 ± 7.16	.942
LV mass index, g/m ²	62.13 ± 10.52	64.78 ± 10.64	62.95 ± 9.28	.392	59.54 ± 11.29	57.26 ± 7.10	.408
Infarct size, % LV mass	24.56 [18.02, 33.94]	22.36 [15.26, 32.78]	26.88 [21.13, 40.60]	.023	23.53 [18.53, 32.50]	32.78 [24.38, 38.88]	.009

CMD, coronary microvascular dysfunction; CMR, cardiac magnetic resonance; IQR, inter-quartile range;

LV, left ventricular; LVEDVi, left ventricular end diastolic volume index; LVEF, left ventricular ejection fraction; LVESVi, left ventricular end systolic volume index; MetS, metabolic syndrome.

Data are presented as mean ± standard deviation, median [interquartile range], or No. (%).

Figure S1. Schoenfeld residual plots for the Cox proportional hazards model in the MetS subgroup.



CMD, coronary microvascular dysfunction; MetS, metabolic syndrome.

Correcciones a la figura

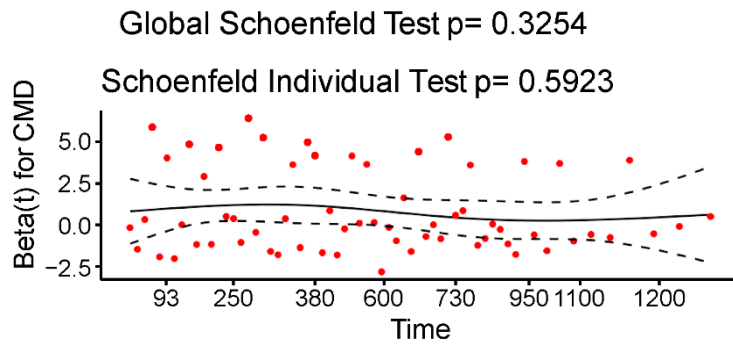
Cambiar "Test" a "test"

Cambiar "Individual Test" a "individual test".

Indicar valores de P en formato REC: $P = .6473$

Eje horizontal: separar 1000 y 1100

Figure S2. Schoenfeld residual plots for the Cox proportional hazards model in the non-MetS subgroup.



CMD, coronary microvascular dysfunction; MetS, metabolic syndrome.

Correcciones a la figura

Cambiar "Test" a "test"

Cambiar "Individual Test" a "individual test".

Indicar valores de P en formato REC: $P = .3254$

REFERENCES

1. Masci PG, Ganame J, Strata E, Desmet W, Aquaro GD, Dymarkowski S, *et al.* Myocardial salvage by CMR correlates with LV remodeling and early ST-segment resolution in acute myocardial infarction. *JACC Cardiovasc Imaging* 2010;**3**:45-51.
2. Li J, Gong Y, Wang W, Yang Q, Liu B, Lu Y, *et al.* Accuracy of computational pressure-fluid dynamics applied to coronary angiography to derive fractional flow reserve: FLASH FFR. *Cardiovasc Res* 2020;**116**:1349-1356.
3. Gong Y, Feng Y, Yi T, Yang F, Li Y, Zhang L, *et al.* Coronary Angiography-Derived Diastolic Pressure Ratio. *Front Bioeng Biotechnol* 2020;**8**:596401.
4. Johnson NP, Kirkeeide RL, Asrress KN, Fearon WF, Lockie T, Marques KM, *et al.* Does the instantaneous wave-free ratio approximate the fractional flow reserve? *J Am Coll Cardiol* 2013;**61**:1428-1435.
5. Choi KH, Dai N, Li Y, Kim J, Shin D, Lee SH, *et al.* Functional Coronary Angiography-Derived Index of Microcirculatory Resistance in Patients With ST-Segment Elevation Myocardial Infarction. *JACC Cardiovasc Interv* 2021;**14**:1670-1684.